NUB-3248/TH-04
DESY 04-031
hep-ph/0403001

FRONTIERS IN COSMIC RAYS*

LUIS A. ANCHORDOQUI
Department of Physics, Northeastern University, Boston, MA 02115, USA
E-mail: l.anchordoqui@neu.edu

CHARLES D. DERMER
Code 7653, Naval Research Laboratory, 4555 Overlook Ave. SW, Washington, DC 20375-5352 USA
E-mail: dermer@gamma.nrl.navy.mil

ANDREAS RINGWALD
Deutsches Elektronen-Synchrotron DESY, D-22603 Hamburg, Germany
E-mail: andreas.ringwald@desy.de

This rapporteur review covers selected results presented in the Parallel Session HEA2 (High Energy Astrophysics 2) of the *10th Marcel Grossmann Meeting on General Relativity*, held in Rio de Janeiro, Brazil, July 2003. The subtopics are: ultra high energy cosmic ray anisotropies, the possible connection of these energetic particles with powerful gamma ray bursts, and new exciting scenarios with a strong neutrino-nucleon interaction in the atmosphere.

1. Introduction

Since the early 60's several ground-based experiments have observed extensive air showers, presumably triggered by ultra high energy cosmic rays (UHECRs) interacting in the upper atmosphere.[1] The highest primary energy measured thus far is $E \sim 10^{20.5}$ eV,[2] corresponding to a center-of-mass energy $\sqrt{s} = \sqrt{2 m_p E} \sim 750$ TeV, where m_p is the proton mass. The interest in the origin of these particles is twofold: there is not only the intellectual curiosity about unknown properties of powerful astrophysical scenarios, but also the possibility to probe new physics at energies beyond the reach of any foreseeable man-made experiments.

Theoretically, one expects the CR spectrum to fall off somewhat above 10^{20} eV, because the particle's energy gets degraded through interactions with the cosmic microwave background (CMB), a phenomenon known as the Greisen-Zatsepin-Kuzmin (GZK) cutoff.[3] Unfortunately, as one can see in Fig. 1, the most recent measurements by the HiRes[4] and AGASA[5] experiments are apparently in conflict, if only statistical errors are taken into account, and the source of the difference remains

*Rapporteur review of HEA2 – 10th Marcel Grossmann Meeting on General Relativity –

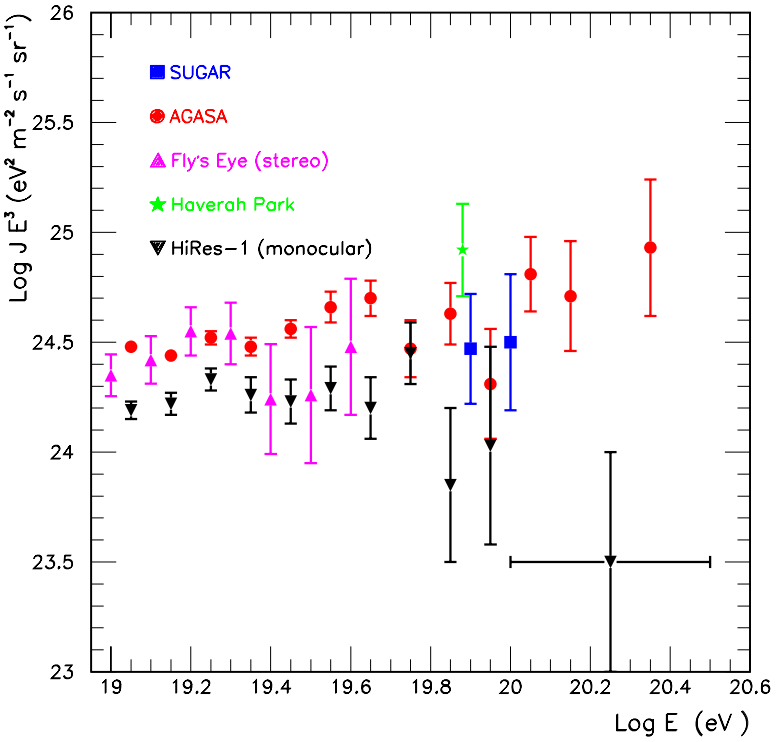

Figure 1. Data on the upper end of the cosmic ray energy spectrum with their statistical error bars. (HiRes,[4] AGASA,[5] Fly's Eye,[6] Haverah Park,[7] and SUGAR.[8])

unknown. However, if one takes the systematic uncertainties in the energy measurements into account, one finds that both data sets are mutually compatible on the $2\,\sigma$ level.[9] Attempts to explain the AGASA data with a homogeneuos population of astrophysical sources that injects power-law distributions of CRs give unacceptable χ^2 (see, e.g., Refs. [10,11,12]). On the other hand, an analysis[13] of the combined data reported by the HiRes, the Fly's Eye, and the Yakutsk collaborations is supportive of the existence of the GZK cutoff at the $> 5\,\sigma$ ($> 3.7\,\sigma$, depending upon the extrapolated energy spectrum) level.[a] The deviation from GZK depends on the set of data used as a basis for power law extrapolation from lower energies. One caveat is a recent claim[15] that there may be technical problems with the Yakutsk data collection. In view of the low statistics at the end of the spectrum and the wide variety of uncertainties in these experiments, perhaps the rational thing to do is to wait for more data, conservatively arguing that the jury is still out.

In this Parallel Session we saw many thorough reviews covering all the most

[a] This evidence disappears, however, if one assumes that UHECRs are protons and excludes nearby ($\lesssim 50$ Mpc) sources from the otherwise homogeneous distribution.[14] In this case even the HiRes-1 data are incompatible with the GZK cutoff on the $3\,\sigma$ level.[10,11]

interesting and timely topics in CR physics. In this rapporteur summary we cannot do justice to all the presentations.[b] Priority will be given to two intriguing scenarios, which pose possible explanations of the data.

2. Anisotropies in UHECRs

At the highest energies, the arrival directions of CRs are expected to begin to reveal their origins. If the CR intensity were isotropic, then one should expect a time-independent flux from each direction in local detector coordinates, i.e., declination and hour angle. In that case, a shower detected with local coordinates could have arrived with equal probability at any other time of a shower detection. For any point of the celestial sphere, the expected shower density can be estimated if the exposure in each direction can be obtained. This implies that celestial anisotropies can be easily discerned by comparing the observed and expected event frequencies at each region.

For experiments with 100 % duty cycle, continuous operation in solar time for several years leads to a uniform observation in right ascension. Therefore, one of the conventional methods to search for any global anisotropy is to apply the Linsley's[17] harmonic analysis to the full sky cosmic ray distribution, i.e., determine the amplitude and phase of the $m^{\rm th}$ harmonic by fitting the right ascension distribution of events to a sine wave with period $2\pi/m$.

There is a remarkable agreement among several experiments favoring a significant anisotropy (encoded in the first harmonic amplitude) around 10^{18} eV from the general direction of the Galactic Plane (GP). Specifically, the AGASA experiment has revealed a correlation between the arrival direction of CRs (with energy $\sim 10^{18}$ eV) and the GP at the $4\,\sigma$ level.[18] The GP excess, which is roughly 4% of the diffuse flux, is mostly concentrated in the direction of the Cygnus region, with a second spot towards the Galactic Center (GC).[19] Evidence at the $3.2\,\sigma$ level for GP enhancement in a similar energy range has also been reported by the Fly's Eye Collaboration.[20] Interestingly, the full Fly's Eye data include a directional signal from the Cygnus region which was somewhat lost in an unsuccessful attempt to relate it to γ-ray emission from Cygnus X-3.[21] Finally, the existence of a point-like excess in the direction of the GC has been confirmed via independent analysis of data collected with the SUGAR experiment.[22]

For the ultra high energy ($> 10^{19.6}$ eV) regime, all experiments to date have reported no departure from isotropy in the first harmonic amplitude.[23c] This does not imply an isotropic distribution, but it merely means that available data are too

[b] A scenario in which UHECRs are able to break the GZK barrier was presented by She-Sheng Xue.[16]

[c] For the Fly's Eye data-sample the first harmonic amplitude is computed using weighted showers, because it has had a nonuniform exposure in sideral time. A shower's weight depends on the hour of its sideral arrival time, and the 24 different weights are such that every time bin has the same weighted number of showers.

sparse to claim a statistically significant measurement of anisotropy. In other words, there may exist anisotropies at a level too low to discern given existing statistics.[24]

The right ascension harmonic analyses are completely blind to intensity variations which depend only on declination. Combining anisotropy searches in right ascension over a range of declinations could dilute the results, since significant but out of phase "Rayleigh vectors" from different declination bands can cancel each other out. Moreover, the analysis methods that consider distributions in one celestial coordinate, while integrating away the second, have proved to be potentially misleading.[25] An unambiguous interpretation of anisotropy data requires two ingredients: *exposure to the full celestial sphere and analysis in terms of both celestial coordinates.*[26]

The first full sky search for large scale anisotropies in the distribution of arrival directions of CRs with energy $> 10^{19.6}$ eV was reported in this Parallel Session by John Swain.[27] Data from the SUGAR and AGASA experiments, taken during a 10 yr period with nearly uniform exposure to the entire sky, show no departures from either homogeneity nor isotropy on angular scale greater than 10°.

In this full-sky anisotropy search, the intensity distribution of the set of $N = 99$ arrival directions

$$I(\mathbf{n}) = \frac{1}{\mathcal{N}} \sum_{j=1}^{N} \frac{1}{\omega_j} \, \delta(\mathbf{n}, \mathbf{n}_j) \ , \tag{1}$$

was conviniently expanded in spherical harmonics ($Y_{\ell m}$)

$$I(\mathbf{n}) = \sum_{\ell=0}^{\infty} \sum_{m=-\ell}^{\ell} a_{\ell m} \, Y_{\ell m}(\mathbf{n}) \ , \tag{2}$$

going into the multipole expansion out to $\ell = 5$. Here, ω_j is the relative exposure at arrival direction $\mathbf{n}_j$ and $\mathcal{N}$ is the sum of the weights ω_j^{-1}. The coordinate independent total power spectrum of fluctuations,

$$C(\ell) = \frac{1}{(2\ell + 1)} \sum_{m=-\ell}^{\ell} a_{\ell m}^2 \ , \tag{3}$$

is consistent with that expected from a random distribution for all (analyzed) multipoles, though there is a small (2σ) excess in the data for $\ell = 3$.[28] To give a visual impression of the level of homogeneity and isotropy in existing data, in Fig. 2 we show the intensity distribution as seen by AGASA and SUGAR experiments.

3. UHECRs from GRBs

In this section, arguments for the origin of UHECRs from gamma ray bursts (GRBs) are reviewed. This line of enquiry has led to a complete model for CRs originating from supernovae (SNe) and GRBs in our Galaxy and throughout the universe,[29,12] which is summarized here.

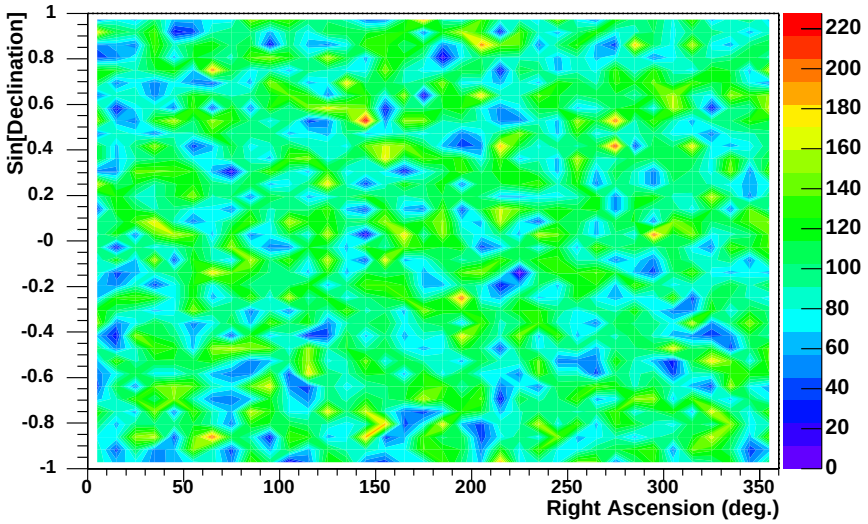

Figure 2. UHECR intensity in arbitrary units (equatorial coordinates) as seen by the AGASA and SUGAR experiments.

The connection betweeen GRBs and UHECRs was first made on the basis of an intriguing coincidence[30,31] beween the power required to sustain the measured flux of super-GZK ($\gtrsim 10^{20}$ eV) CRs against photohadronic energy losses and the local time- and space-averaged hard X-rays/soft γ-ray luminosity of GRBs. This luminosity density is estimated to be $\approx 10^{44}$ ergs Mpc^{-3} yr^{-1}. Thus GRBs have, in principle, sufficient energy to power the UHECRs and post-GZK CRs. Moreover, many GRB sources are found within the GZK radius, and CRs with energies $\gtrsim 10^{20}$ eV can be accelerated by the relativistic shocks formed in GRB explosions.[32] The hypothesis of a GRB/UHECR association points to a closer connection between SNe and CRs that could provide a complete solution to the problem of CR origin.

3.1. *CRs from Supernovae*

Even though the controversy surrounding the origin of the UHECRs has generated much interest, it should be noted that the much older problem of the origin of the CRs is itself not solved. Cosmic rays with energies from GeV/nucleon up to hundreds of TeV are widely thought to be accelerated by supernova remnant (SNR) shocks. Yet the prediction that SNRs should be luminous γ-ray sources and display the characteristic 70 MeV π^0 decay emission feature from hadronic interactions was not confirmed by the EGRET instrument on the *Compton Observatory*. Nevertheless, there is statistical evidence that SNRs are associated with unidentified γ-ray sources.[33] There is also clear evidence for a π^0 decay feature in the diffuse galactic γ-ray background, even if the spectrum is harder than would be expected if CRs throughout the Galaxy have the same spectrum as those observed locally.[34]

There is also some evidence from Cas A that the TeV emission originates from hadronic interactions,[35] though at a much lower level than would be expected if SNRs accelerated CRs with $\sim 10\,\%$ efficiency.

These clues suggest that the solution to the CR problem below the knee of the CR spectrum at ≈ 3 PeV and, indeed, the problem of the origin of CRs at all energies, might be a consequence of the diversity in the types of supernovae (SNe). SNe are hardly uniform: the simplest separation is between the explosively burning white dwarfs (Type Ia), and the core collapse SNe (Type II and Types Ib and Ic). Moreover, the ejecta speeds vary greatly,[36] from a few thousand km per second in Type II SNe with massive H envelopes, to speeds of $\approx 10^5$ km/s in Type Ib/c SNe where the H and He envelopes have been lost either to stellar winds or to Roche lobe overflow to a binary companion.

The discovery that the GRBs which are observed today took place at cosmological distances led to the development of the relativistic fireball/blast-wave model[37] that generalizes the theory of SNe to stellar explosions with relativistic ejecta. The coasting Lorentz factors of GRB outflows reach values of 10^2 – 10^3. Associated with this discovery are other far-reaching observational results[38] that tie GRBs to a subset of SNe: GRBs are associated with massive stars in star-forming galaxies; optically dark GRBs could be due to extreme reddening from large quantities of dust and gas, as found in molecular cloud complexes where massive stars are born; and delayed reddened excesses in the late-time optical afterglow light curves appear to be SN emissions, and can often be fit with a template light curve of the Type Ib/c SN 1998bw.

A final important discovery is that GRB outflows are in the form of highly collimated jets. The evidence for beaming is inferred from beaming breaks in optical afterglow light curves that occur when the Doppler cone of the decelerating relativistic outflow is about the same size as the jet cone. From the beaming breaks, one can infer that the mean solid angle subtended by a GRB jet is about 1/500th of the full sky.[39] As a consequence, there are many hundreds of GRBs events that take place for every one that is observed. By performing the statistics of GRB sources, one finds that the rate of GRBs in the Milky Way reaches $\approx 10\%$ of the rate of Type 1b/c SNe. All these lines of evidence suggest that GRBs are a species of SNe.

3.2. *CRs from GRBs*

What does this mean for a complete model of cosmic rays? It is not sufficient to provide an explanation for CRs with energies $\gtrsim 10^{18}$ eV without at least speculating on the origin of CRs with energies from the knee to the ankle. Many explanations have been suggested, including CR production from pulsars or extremely energetic SNe in the Galaxy, acceleration at the Galactic wind termination shock, or extragalactic models where CRs above the knee diffuse into the Galaxy.[40] A complete explanation based on acceleration in SNe shocks would tie our understanding of CR acceleration by SNe at GeV – TeV energies with an origin of UHECRs in the

relativistic shocks associated with GRB SNe.

In the model of Ref. [12], high-energy cosmic rays (HECRs), defined as those with energies $\gtrsim 10^{14}$ eV, are assumed to be accelerated at the shocks produced by the Type Ib/c SNe that collapse to form GRBs. From the evidence for beaming and the association of GRBs with star-forming galaxies like the Milky Way, GRB events are estimated to occur once every 3000 – 10000 yrs in the Galaxy. Relativistic shock acceleration in GRB blast waves are assumed to inject power-law spectra of ions from a minimum energy $E_{\rm min} \approx 10^{14}$ eV to a high-energy cutoff $E_{\rm max} \gtrsim 10^{20}$ eV. HECRs injected in the Milky Way diffuse and escape from our Galaxy, and UHECRs with energies $\gtrsim 10^{17}$ – 10^{18} eV that have Larmor radii comparable to the size scale of the halo escape directly from the Milky Way and propagate almost rectilinearly through extragalactic space. By the same token, UHECRs produced from other galaxies can enter the Milky Way to be detected. UHECRs formed in GRBs throughout the universe travel over cosmological distances and have their spectrum modified by energy losses, so an observer in the Milky Way will measure a superposition of UHECRs from extragalactic GRBs and HECRs produced in our Galaxy.

The model of Ref. [12] fits the measured KASCADE[41] spectra of HECRs in the knee region, and the HiRes data[4] at ultra-high energies. The fits imply the HECR injection spectral index and luminosity function of GRBs. The results show that GRBs must be strongly baryon-loaded, with the testable prediction that GRBs will produce a detectable number of high energy neutrino showers in a km-scale neutrino detector such as IceCube.

3.3. *GRB Model for HE and UHECRs*

High energy CRs from a GRB in the Galaxy are assumed to propagate diffusively as a result of pitch-angle scattering with magneto-hydrodynamical (MHD) turbulence superposed on the Galactic magnetic field.[12,42] The Larmor radius $r_{\rm L}$ of a CR propagating in a magnetic field of strength $B_{\mu{\rm G}} \equiv 1\mu$G is $\cong A\gamma_6/(ZB_{\mu{\rm G}})$ pc, where $\gamma = 10^6\,\gamma_6$ is the Lorentz factor of a CR with atomic mass A and charge Ze. The mean-free-path λ between pitch-angle scatterings of a CR with Larmor radius r_L is assumed to be inversely proportional to the energy density in the MHD spectrum at wave-number $k \sim r_L^{-1}$. A two-component turbulence spectrum is assumed with wave-number index $q = 3/2$ for a Kraichnan-type spectrum at small wave number, and index $q = 5/3$ for a Kolmogorov-type spectrum at large wave numbers. The two components give a Z-dependent break in the scattering mean-free-path λ at energy $E_Z\,({\rm PeV}) \cong ZB_{\mu{\rm G}}b_{\rm pc}$, where we take $B_{\mu{\rm G}} = 3$, and find that $b_{\rm pc} = 1.6$ is the wavelength in parsecs of the MHD waves where the spectrum changes from Kraichnan to Kolmogorov turbulence. The injection of turbulence at large wave numbers is probably due to SN explosions in the Galaxy; the small wave number turbulence could be a consequence of halo/disk interactions (e.g., high-velocity clouds passing through the Galaxy's disk).

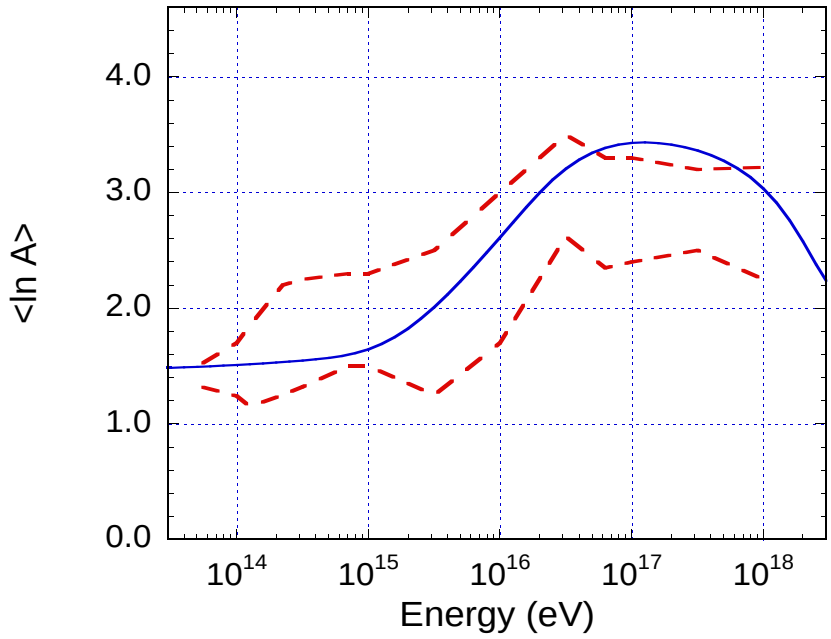

Figure 3. Solid curve shows the value of $\langle \ln A \rangle$ calculated from the model of Wick, Dermer, and Atoyan (2004), where a single GRB in the Galaxy releases 10^{52} ergs in the form of a power-law spectrum of CRs with energies between $\approx 10^{14}$ eV and 10^{20} eV. In the model, a Galactic GRB occurred 2.1×10^5 years ago at a distance of 500 pc from Earth. The CRs isotropically diffuse via pitch-angle scattering with an energy-dependent mean-free-path λ determined by the MHD turbulence spectrum. The dashed curves outline the expected range of uncertainty in $\langle \ln A \rangle$ from the experimental data and our knowledge of particle physics[40]. The effect on $\langle \ln A \rangle$ of extragalactic CRs at energies $\gtrsim 10^{17}$ is not included.

The diffusion radius $r_{\rm dif} \cong 2\sqrt{\lambda ct/3}$. When $r \ll r_{\rm dif}$, the HECR differential number density $n(\gamma; r, t) \propto t^{-3/2} \times \gamma^{-p-3(2-q)/2}$. The measured spectrum is steepened by $\frac{3}{2}(2-q)$ units because the diffusion coefficient $D \propto \lambda \propto \gamma^{2-q}$ for an impulsive source.[43] An injection spectrum with $p = 2.2$, as expected from relativistic shock acceleration, gives a measured spectrum $n_{Z,A}(\gamma; r, t) \propto \gamma^{-s}$, with $s = 2.7$ at $E \ll E_Z$ and $s = 2.95$ at $E \gg E_Z$. These indices are similar to the measured CR indices below and above the knee energy.

Figure 3 shows the predicted mean logarithmic mass $\langle \ln A \rangle$ for CRs which diffuse from a GRB that occurred 2.1×10^5 years ago at a distance of 500 pc from Earth. For comparison, the range of $\langle \ln A \rangle$ derived from direct measurements using a phenomenological model of particle interactions is shown.[40] As can be seen, the model gives a good fit to the data at energies $\ll 10^{17}$ eV, which is expected because the model also provides good fits to the individual spectra of CR ions measured with KASCADE. The model displays an excess abundance of heavy ions at higher ener-

gies, but the calculated value of $\langle \ln A \rangle$ shown here does not include contributions from extragalactic CRs, which become important above $\gtrsim 10^{17}$ eV (see Fig. 4). If the extragalactic component is primarily CR protons, then this discrepancy is resolved.

Good fits to knee data were obtained with a break in the turbulence spectrum at wave numbers corresponding to $\approx$ 1 pc. Composition enhancements by a factor of 50 and 20 for C and Fe, respectively, over Solar photospheric abundances are also required. The likelihood for such an event is reasonable, and the corresponding anisotropy of the CRs from a single source is shown to be consistent with observations.[12]

UHECRs produced by GRBs throughout the universe lose energy adiabatically during the expansion of the universe, and through photo-pair and photo-pion production on the CMB. The loss processes produce features in the UHECR flux from distant ($z \gtrsim 1$) GRB sources at characteristic energies $\sim 4 \times 10^{18}$ eV and $\sim 5 \times 10^{19}$ eV from photo-pair and photo-pion processes, respectively. Comparison of the integrated and evolved UHECR spectrum with data depends on how the luminosity density of GRB sources evolve through cosmic time. In view of the evidence that GRBs are associated with massive stars, the GRB luminosity density is assumed to be proportional to the star formation rate (SFR) history of the universe as traced by the blue and UV luminosity density of distant galaxies. The lowest possible SFR is expected to follow the evolution of the observed optical/UV luminosity density, and a higher rate to follow this rate with allowance for extinction corrections.[44]

Figure 4 shows the best fit model to the all-particle spectrum from below the knee of the CR spectrum to the highest energies. The best fit model to the data has an injection index $p = 2.2$, a high-energy exponential cutoff energy of 10^{20} eV, and a SFR which follows the higher extinction-corrected rate. The transition between galactic and extragalactic CRs is found in the vicinity of the second knee ($10^{17.6}$ eV), consistent with a heavy-to-light composition change.[45] The ankle ($10^{18.5}$ eV) is interpreted as a suppression from photo-pair losses, analogous to the GZK suppression at higher energies.

Fits to the data define the local luminosity density of GRBs for producing HECRs. The GRB HECR luminosity density is found to be $\cong 70 \times 10^{44}$ erg Mpc^{-3}yr^{-1}, so that this model implies that GRBs inject considerably more energy in the form of nonthermal hadrons than electrons. Thus GRB blast waves are baryon-loaded by a factor $\approx 60 - 100$ compared to the energy radiated by GRBs in the form of hard X-ray and soft γ-ray emission. For the large baryon load required for this model, calculations show that 100 TeV – 100 PeV neutrinos could be detected several times per year from all GRBs with kilometer-scale neutrino detectors such as IceCube.[12,46] Detection of even 1 or 2 neutrinos from GRBs with IceCube or a northern hemisphere neutrino detector would unambiguously demonstrate the high nonthermal baryon load in GRBs, and would provide compelling

10

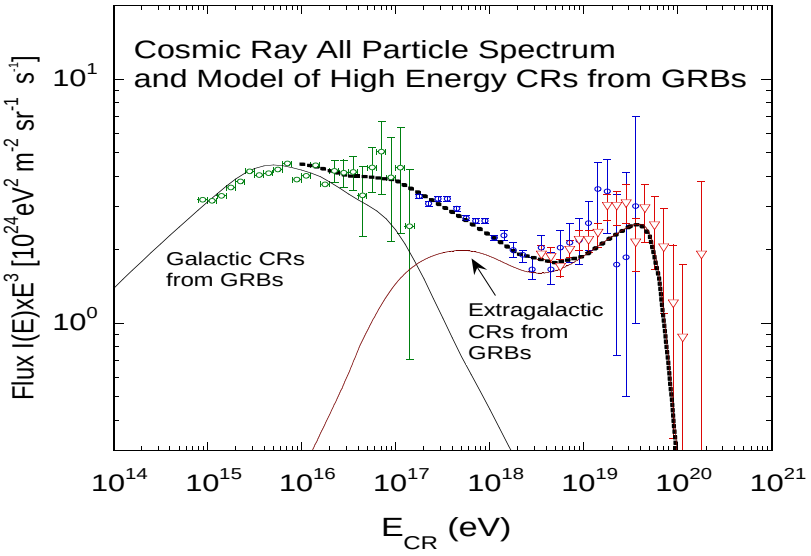

Figure 4. Fit of the model of Ref. [12] to the KASCADE ($< 2 \times 10^{17}$ eV), HiRes-II Monocular (circles), and HiRes-I Monocular (inverted triangles) data, assuming that GRBs inject a power law distribution of particles with index $p = 2.2$ from 10^{14} eV to a maximum energy with an exponential cutoff at $E_{\rm max} = 10^{20}$ eV. A minimum χ^2 routine was used to find the best fit model which has a $\chi^2_r = 1.03$. This fit implies that the transition from Galactic to extragalactic CRs occurs near the second knee at $10^{17.6}$ eV, and that the ankle ($10^{18.5}$ eV) is a feature associated with photo-pair production. The heavy dark points shows the best fit model, and the galactic and extragalactic components are shown separately.

support for this scenario for the origin of CRs.

Finally, we note that these calculations have implicitly assumed that the Fly's Eye/HiRes measurements of the UHECR spectrum are correct. If a post-GZK excess is confirmed, then physics beyond the standard model could be required, as discussed in Sec. 4.

3.4. *The Last GRB in the Galaxy and the CR Excess from the GC*

As discussed in Sec. 2, the AGASA[18] and the SUGAR[22] experiments observed an excess of CRs from the direction of the GC. The SUGAR data suggest a point source to within their spatial resolution, while AGASA shows an extended source. The excess starts to be significant around $10^{17.5}$ eV, peaks near 10^{18} eV, and cuts off sharply at about $10^{18.5}$ eV. The flux of the excess particles represents a luminosity of particles beyond 10^{18} eV of about 4×10^{30} erg/s. The GC anisotropy is then very suggestive of neutrons as candidate primaries, because the directional signal requires relatively-stable neutral primaries, and time-dilated neutrons can reach the Earth from typical Galactic distances when the neutron energy exceeds 10^{18} eV.

A novel hypothesis to explain the GC excess involving GRBs was presented in this Parallel Session by Gustavo Medina Tanco.[47] In order to estimate the remaining

traces of any CR activity produced by the last GRB in the galaxy, one has to take into account several considerations:
(i) The UHECRs escaping the GRB fireball

$$N_0(E > 10^{18}\ \mathrm{eV}) \sim 10^{-2}\ N_0(E > E_{\min}) \tag{4}$$

are mostly neutrons, because protons are captive in the magnetic field and suffer extensive adiabatic losses on the way out.[48d] Some of these neutrons will decay into protons within the GC thin disk-like ($r \sim 3$ kpc) region of high interstellar medium density and high star formation rate. The population of secondary protons would then be captured by the strong B-field near the GC, attaining diffusion with a residence time scale of about $T \sim 10^5$ yr. At the end of this time, about 1/300 protons are able to avoid leakeage. The trapped protons,

$$N_T(E > 10^{18}\ \mathrm{eV}) = N_0(E > 10^{18}\ \mathrm{eV})\ \left(1 - e^{-\frac{r\, m_n}{E\, \overline{\tau}}}\right)/300\ , \tag{5}$$

can then be turned back into neutrons by interaction with nuclei in the interstellar medium with probability of 5×10^{-2}. Here, m_n and $\overline{\tau}$ are the neutron mass and lifetime, respectively.
(ii) The formation of the $n \to p$ reservoir depends on the GRB rate in the inner Galaxy times the probability that a GRB jet points more o less along the direction of the GP. The latter is estimated to be about 50 %.
(iii) The total CR production by a single GRB is $\approx 10^{51}$ erg.[49]

Putting all this together, the observed anisotropy in the direction of the GC can be easily fitted by the neutrons produced in the GRB reservoir, that ultimately travel unscathed to Earth.[50] Arguably, if the anisotropy messengers are neutrons, then those with energies below 10^{18} eV will decay in flight, providing a flux of cosmic antineutrinos above 1 TeV that should be observable at kilometer-scale neutrino telescopes.[51]

3.5. *UHECRs, EMBHs, and GRBs*

An alternative explanation for the GRB phenomenon has been recently put forward.[52] In this model the GRB explosion is due to the rapid discharge of an electromagnetic black hole (EMBH). This chain reaction occurs when a massive star collapses into an EMBH able to produce a dyadosphere, i.e., the EMBH reaches the critical field for the Schwinger process, $\mathcal{E}_c = m_e^2 c^3/\hbar e \simeq 1.3 \times 10^{18}$ V/m.[53] The $e^{\pm}$ pairs created through vacuum polarization then promptly annihilate into the GRB. This model explains the time variability, the spectra, and the GRB afterglows to a very high level of accuracy.[54] Based on the EMBH-GRB hypothesis, in this Parallel Session Alvise Mattei[55] presented a mechanism to accelerate the ionized hydrogen atoms surrounding the death star to ultra high energies.

[d] We remind the reader that the differential injection spectrum of GRBs $\propto E^{-2.2}$.

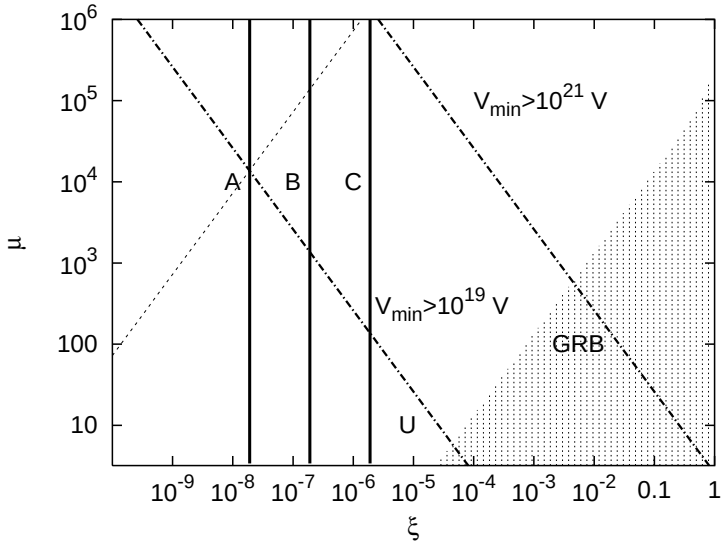

Figure 5. Limits on charge and mass ratio for UHECR emission. EMBHs lying in the shaded zone develop a dyadosphere. EMBHs above the dotted line cannot activate the ionization mechanism. EMBHs on the right hand side of the dashed-dotted lines produce particles at lower energies between 10^{19} eV and 10^{21} eV. The vertical solid lines indicate the maximum energy limit for proton acceleration, A, B, and C corresponds to $E_{\rm max} > 10^{19}$ eV, $E_{\rm max} > 10^{20}$ eV, and $E_{\rm max} > 10^{21}$ eV; respectively. (This figure is courtesy of Alvise Mattei).

In this set-up protons would be accelerated outward in a very short time along a straight line by the induced electric field. Larmor losses would overcome gains if the energy increases as $dE/dx \sim 10^{21}$ MeV/m. Thus, protons do not suffer catastrophic energy losses if the EMBH cannot produce a dyadosphere. In terms of the mass $M_{\rm BH}$ and the charge $Q_{\rm BH}$ of the BH, the condition for dyadosphere formation near the BH horizon (of radius $r_{\rm H}$), $\mathcal{E}(r_{\rm H}) < \mathcal{E}_c$, is found to be

$$\mu < 6 \times 10^5 \, \xi \, \left(1 + \sqrt{1-\xi^2}\right)^{-2} \tag{6}$$

where $\mu \equiv M_{\rm BH}/M_\odot$ and $\xi \equiv Q_{\rm BH}/Q_{\rm max}$. In order to produce a baryon reservoir, the electromagnetic field has to be able to ionize hydrogen atoms, i.e., a ionization potential of 13.6 V must be active in a distance of about a Bohr radius. This condition can be re-written as $\mathcal{E}(r_{\rm H}) \gtrsim 2.5 \times 10^{11}$ V/m, or equivalently

$$\mu \leq 2.9 \times 10^{12} \, \xi \, \left(1 + \sqrt{1-\xi^2}\right)^{-2} \, . \tag{7}$$

The limits impossed by these constraints are summarized in Fig. 5.

In summary, an EMBH would lose its charge by emitting UHECRs if the BH does not reach the the critical charge-to-mass ratio given in Eq. (6). This type of BH has been classified as pure or U-EMBH. The BH population that has recently exploded as a GRB ends up near the dyadosphere zone with residual charge, and so UHECR emission is still possible until complete discharge.

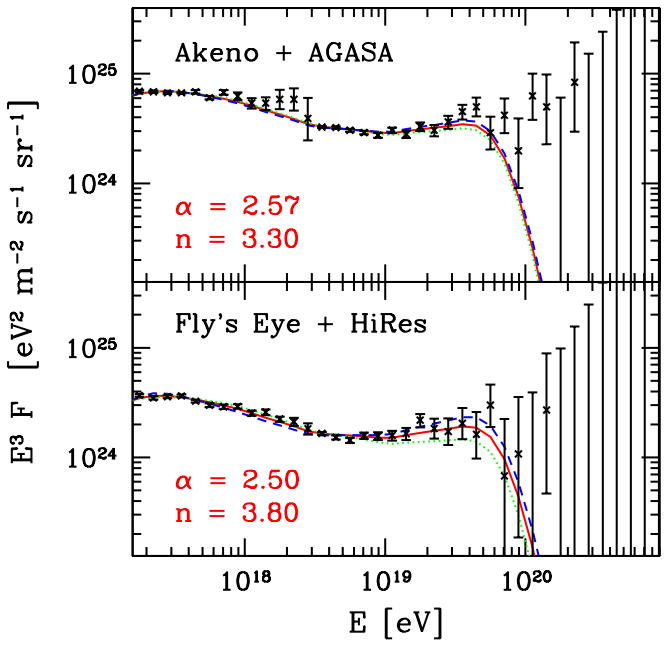

Figure 6. Ultrahigh energy cosmic ray data with their statistical errors (top: combination of Akeno[56] and AGASA[57] data; bottom: combination of Fly's Eye[45] and HiRes[58] data) and the predictions arising from a power-law emissivity distribution (8) corresponding to sources which are uniformly distributed at cosmological distances. The best fits between $E_- = 10^{17.2}$ eV and $E_+ = 10^{20}$ eV are given by the solid lines and correspond to the indicated values of the parameters α and n in the source emissivity distribution. The 2-sigma variations corresponding to the minimal (dotted) and maximal (dashed) fluxes are also shown. Other parameters of the analysis were $E_{\rm max} = 3 \times 10^{21}$ eV, $z_{\rm min} = 0.012$, and $z_{\rm max} = 2$. From Ref. [11].

4. Strongly Interacting Neutrinos

We have noted in the Introduction that if the highest energy cosmic rays are nucleons (or nuclei), if their sources are indeed uniformly distributed at cosmological distances, and if their injection spectra are power-laws in energy – a reasonable assumption, in view of the measured spectrum in Fig. 4 which appears to be approximately of (broken) power-law type over many order of magnitude in energy – then their total flux arriving at Earth should show a pronounced drop above the GZK cutoff $E_{\rm GZK} \approx 4 \times 10^{19}$ eV (1×10^{20} eV, for nuclei). This is due to the fact that, above this energy, the universe becomes opaque to high energy nucleons (and nuclei), due to inelastic hadronic scattering processes with the CMB photons. The GZK cutoff is, however, not seen in the data, at least not in a significant manner (cf. Fig. 6). Correspondingly, the events above 10^{20} eV in Fig. 6 should originate from small distances below 50 Mpc, the typical interaction length of nucleons above $E_{\rm GZK}$. However, no source within a distance of 50 Mpc is known in the arrival directions of the post-GZK events. The basic puzzle is: if there are no large inter-

vening magnetic fields and the sources of ultrahigh energy cosmic rays are indeed at cosmological distances, how could they reach us with energies above 10^{20} eV?

At the relevant energies, among the known particles only neutrinos can propagate without significant energy loss from cosmological distances to us. This fact leads naturally to scenarios invoking hypothetical – beyond the Standard Model of elementary physics – strong interactions of ultrahigh energy cosmic neutrinos,[59] whose modern incarnation we review in this section.[60]

Such scenarios are based on the observation that the flux of neutrinos originating from the decay of the pions produced during the propagation of nucleons through the CMB[59,61] – the cosmogenic neutrinos – shows a nice agreement with the observed UHECR flux above $E_{\rm GZK}$. Assuming a large enough neutrino-nucleon cross-section at these high energies, these neutrinos could initiate extensive air showers high up in the atmosphere, like hadrons, and explain the existence of the post-GZK events.[59] This large cross-section is usually ensured by new types of TeV-scale interactions beyond the Standard Model, such as arising through gluonic bound state leptons,[62] through TeV-scale grand unification with leptoquarks,[63] through Kaluza-Klein modes from compactified extra dimensions,[64] (see, however, Ref. [65]), or through p-brane production in models with warped extra dimensions[66] (see, however, Ref. [67]); for earlier and further proposals, see Ref. [68] and Ref. [69], respectively.

In Refs. [10,60], a detailed statistical analysis of the agreement between observations and predictions from such scenarios was presented. Moreover, an example was emphasized which – in contrast to previous proposals – is based entirely on the Standard Model of particle physics. It exploits non-perturbative electroweak instanton-induced processes for the interaction of cosmogenic neutrinos with nucleons in the atmosphere, which may have a sizeable cross-section above a threshold energy $E_{\rm th} = \mathcal{O}((4\pi m_W/\alpha_W)^2)/(2m_p) = \mathcal{O}(10^{18})$ eV, where m_W denotes the W-boson mass and α_W the electroweak fine structure constant.[70,71,72]

The scenario is based on the assumption of a power-law emissivity distribution corresponding to uniformly distributed sources and thus quite consistent with the GRB model of CR origin from Sec. 3.3. The emissivity is defined as the number of protons per co-moving volume per unit of time and per unit of energy, injected into the CMB with energy E_i and characterized by a spectral index α and a redshift (z) evolution index n,

$$\mathcal{L}_p = j_0\, E_i^{-\alpha}\; (1+z)^n\; \theta(E_{\rm max} - E_i)\, \theta(z - z_{\rm min})\, \theta(z_{\rm max} - z)\;. \qquad (8)$$

Here, j_0 is a normalization factor, which will be fixed by the observed flux. The parameters $E_{\rm max}$ and $z_{\rm min/max}$ have been introduced to take into account certain possibilities such as the existence of a maximal energy, which can be reached through astrophysical accelerating processes in a bottom-up scenario, and the absence of nearby/very early sources, respectively. They turn out to be quite insensitive to the specific choice for $E_{\rm max}$, $z_{\rm min}$, and $z_{\rm max}$, within their anticipated values. The main sensitivity arises from the spectral parameters α and n, for which 1 and $2\,\sigma$

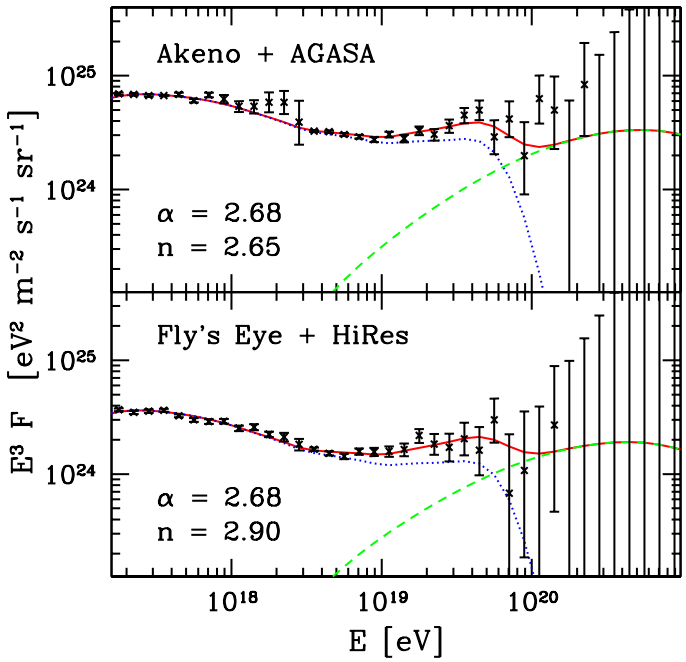

Figure 7. Ultrahigh energy cosmic ray data (Akeno + AGASA on the upper panel and Fly's Eye + HiRes on the lower panel) and their best fits (solid) within the electroweak instanton scenario, for $E_{\max} = 3 \times 10^{22}$ eV, $z_{\min} = 0.012$, $z_{\max} = 2$, consisting of a proton component (dotted) plus a cosmogenic neutrino-initiated component (dashed). From Ref. [10].

confidence regions have been determined. Note, that $n \sim 3, z_{\max} \sim 2$ mimicks the SFR history of the universe mentioned also in connection with GRBs in Sec. 3.3.

After propagation through the CMB, the protons from Eq. (8) will have energies below $E_{\rm GZK}$, so they can well describe the low energy part of the UHECR spectrum. The cosmogenic neutrinos interact with the atmosphere and thus give a second component to the UHECR flux, which describes the high energy part of the spectrum. The relative normalization of the proton and neutrino fluxes is fixed in this scenario, so the low and high energy parts of the spectrum are explained simultaneously without any extra normalization. Details of this analysis can be found in Ref. [10].

Figure 7 shows the best fits for the AGASA and for the HiRes UHECR data. The best fit values are $\alpha = 2.68(2.68)$ and $n = 2.65(2.9)$, for AGASA (HiRes), within the electroweak instanton scenario. One can see very nice agreement with the data within an energy range of nearly four orders of magnitude. The fits are insensitive to the value of $E_{\max}$ as far as one chooses a value above $\approx 3 \times 10^{21}$ eV. The maximum injection energy, however, is constrained by EGRET measurements of the diffuse gamma ray flux.[73] This is because the photons produced via π^0 decay

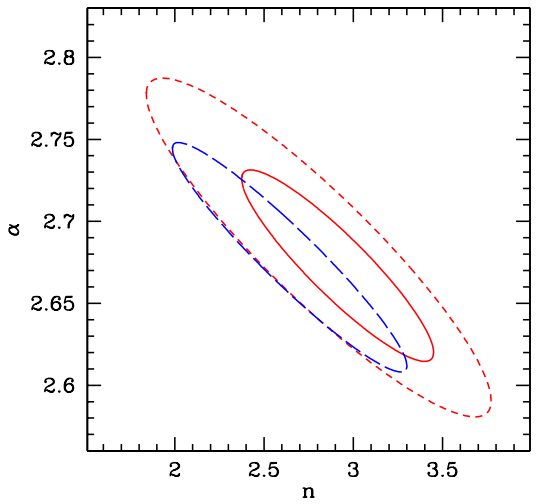

Figure 8. Confidence regions in the α–n plane for fits to the Akeno + AGASA data (2-sigma (long dashed)) and to the Fly's Eye + HiRes data (1-sigma (solid); 2-sigma (short-dashed)), respectively, within the electroweak instanton scenario, for $E_{\rm max} \gtrsim 3 \times 10^{21}$ eV, $z_{\rm min} \geq 0$, $z_{\rm max} = 2$. From Ref. [10].

are degraded in energy due to interactions with the universal radition backgrounds. It is noteworthy that the use of a 2-component model allows $E_{\rm max} \approx 3 \times 10^{22}$ eV without violating the new EGRET bounds.[74]

The shape of the curve between 10^{17} eV and 10^{19} eV is mainly determined by the redshift evolution index n. At these energies the universe is already transparent for protons created at $z \approx 0$, while protons from sources with larger redshift accumulate in this region. The more particles are created at large distances – i.e. the larger n is – the stronger this accumulation should be. In this context, on may note that the data seem to confirm the implicit assumption that the extragalactic uniform UHECR component begins to dominate over the galactic one already at $\approx 10^{17}$ eV. If one, alternatively, starts the fit only at $10^{18.5}$ eV – corresponding to the assumption that the galactic component dominates up to this energy – one finds, however, also a very good fit, with a very mild dependence on n and the same best fit values for α, with a bit larger uncertainties. The peak around 4×10^{19} eV in Fig. 7 shows the accumulation of particles due to the GZK effect. Neutrinos start to dominate over protons at around 10^{20} eV.

Figure 8 displays the confidence regions in the (α,n) plane for AGASA and HiRes. The scenario is consistent on the 2-sigma level with both experiments. For HiRes, the compatibility is even true on the 1-sigma level. It is important to note that both experiments favor the same values for α and n, demonstrating their mutual compatibility on the 2-sigma level (see also Ref. [9]). If one ignores the energy uncertainty in the determination of the goodness of the fit, they turn out to be inconsistent.

Finally, let us emphasize that the same fit results are valid for all strongly interacting neutrino scenarios, as long as the neutrino-nucleon cross-section has a threshold-like behavior as in the case of electroweak instanton-induced processes, with a neutrino threshold energy $\lesssim 4 \times 10^{19}$ eV and a cross-section $\gtrsim 1$ mb above threshold. It is also important to note that the energy requirements on the sources of the primary protons are comparatively mild. To obtain a good fit, one needs $E_{\rm max} \gtrsim 3 \times 10^{21}$ eV. There are several astrophysical source candidates with CR-emission up to this energy;[1] notably, as we discussed in Sec. 3, GRBs can provide the necessary conditions to accelerate protons to the required energies by conventional shock acceleration. Moreover, they naturally provide the power-law source emissivity distribution assumed in Eq. (8).

The predicted ultrahigh energy cosmic neutrino component can be experimentally tested at cosmic ray facilities by studying the zenith angle dependence[71,75] of the events in the range 10^{18} – 10^{20} eV and by analyzing possible correlations with distant astrophysical sources. Additionally, one can look for bumps in neutrino-initiated shower spectra at neutrino telescopes such as IceCube.[76] As laboratory tests, one may search for enhancements in (quasi-)elastic lepton-nucleon scattering[77] or for signatures of QCD instanton-induced processes in deep-inelastic scattering,[78] e.g. at HERA.[79]

In summary, strongly interacting neutrino scenarios provide a viable and attractive solution to the UHECR puzzle and may be subject to various crucial tests in the foreseeable future.

5. Concluding Remarks

We have reviewed some of the interesting ideas currently invoked to explain the origin of UHECRs. We expect future CR experiments, such as the Pierre Auger Observatory,[80] would clarify the confusing experimental situation and shed light on validity of models discussed in this report.

The Pierre Auger Observatory is designed to measure the energy and arrival direction of UHECRs with unprecedented precision. It will consist of two sites, one in the Northern hemisphere and one in the Southern, each covering an area $S \approx 3000$ km^2. The Southern site is currently under construction while the Northern site is pending. Once complete, these two sites together will provide the full sky coverage and well matched exposures which are crucial for anisotropy analyses. The base-line design of the detector includes a ground array consisting of 1600 water Čerenkov detectors overlooked by 4 fluorescence eyes. The angular and energy resolutions of the ground arrays are typically less than 1.5° and less than 20%, respectively. The detectors are designed to be fully efficient out to $\theta_{\rm max} = 60°$ beyond 10^{19} eV. In 10 yr of running the two arrays will collect ≈ 4000 events above $10^{19.6}$ eV. Such statistics will enable us to solve the GZK puzzle.

Acknowledgments

We would like to thank Mario Novello, Santiago Perez Bergliaffa and Remo Ruffini for this very fruitful conference. The work of LAA has been partially supported by the US National Science Foundation (NSF) under grant No. PHY-0140407. The work of CDD is supported by the Office of Naval Research and *GLAST* Science Investigation Grant No. DPR-S-1563-Y.

References

1. See *e.g.,* L. Anchordoqui, T. Paul, S. Reucroft and J. Swain, *Int. J. Mod. Phys.* A **18**, 2229 (2003).
2. D. J. Bird *et al.*, *Astrophys. J.* **441**, 144 (1995).
3. K. Greisen, *Phys. Rev. Lett.* **16**, 748 (1966); G. T. Zatsepin and V. A. Kuzmin, *JETP Lett.* **4**, 78 (1966) [*Pisma Zh. Eksp. Teor. Fiz.* **4**, 114 (1966)].
4. T. Abu-Zayyad *et al.* [High Resolution Fly's Eye Collaboration], astro-ph/0208301.
5. M. Takeda *et al.*, *Astropart. Phys.* **19**, 447 (2003).
6. D. J. Bird *et al.* [HIRES Collaboration], *Astrophys. J.* **424**, 491 (1994).
7. M. Ave, J. Knapp, J. Lloyd-Evans, M. Marchesini and A. A. Watson, *Astropart. Phys.* **19**, 47 (2003).
8. L. Anchordoqui and H. Goldberg, *Phys. Lett.* B, in press [hep-ph/0310054].
9. D. De Marco, P. Blasi and A. V. Olinto, *Astropart. Phys.* **20**, 53 (2003).
10. Z. Fodor, S. D. Katz, A. Ringwald and H. Tu, *Phys. Lett.* B **561**, 191 (2003).
11. Z. Fodor, S. D. Katz, A. Ringwald and H. Tu, *JCAP* **0311**, 015 (2003).
12. S. D. Wick, C. D. Dermer and A. Atoyan, *Astropart. Phys.*, in press [astro-ph/0310667].
13. J. N. Bahcall and E. Waxman, *Phys. Lett.* B **556**, 1 (2003).
14. M. Kachelriess, D. V. Semikoz and M. A. Tortola, *Phys. Rev.* D **68**, 043005 (2003).
15. A. A. Watson, Proc. 28th International Cosmic Ray Conference (Tsukuba), 373 (2003).
16. S. S. Xue, in these Proceedings. See also, hep-ph/0207046.
17. J. Linsley, *Phys. Rev. Lett.* **34**, 1530 (1975).
18. N. Hayashida *et al.* [AGASA Collaboration], *Astropart. Phys.* **10**, 303 (1999).
19. M. Teshima *et al.*, Proc. 27th International Cosmic Ray Conference, (Copernicus Gesellschaft, 2001) p.341.
20. D. J. Bird *et al.* [Fly's Eye Collaboration], *Astrophys. J.* **511**, 739 (1999).
21. G. L. Cassiday *et al.*, *Phys. Rev. Lett.* **62**, 383 (1989).
22. J. A. Bellido, R. W. Clay, B. R. Dawson and M. Johnston-Hollitt, *Astropart. Phys.* **15**, 167 (2001).
23. D. M. Edge, A. M. Pollock, R. J. Reid, A. A. Watson and J. G. Wilson, *J. Phys.* G **4**, 133 (1978); M. M. Winn, J. Ulrichs, L. S. Peak, C. B. Mccusker and L. Horton, *J. Phys.* G **12**, 675 (1986); G. L. Cassiday *et al.*, *Astrophys. J.* **351**, 454 (1990); M. Takeda *et al.*, *Astrophys. J.* **522**, 225 (1999).
24. N. W. Evans, F. Ferrer and S. Sarkar, *Astropart. Phys.* **17**, 319 (2002).
25. J. Wdowczyk and A. W. Wolfendale, *J. Phys.* G **10**, 1453 (1984).
26. P. Sommers, *Astropart. Phys.* **14**, 271 (2001).
27. J. D. Swain, in these Proceedings [astro-ph/0401632].
28. L. A. Anchordoqui, C. Hojvat, T. P. McCauley, T. C. Paul, S. Reucroft, J. D. Swain and A. Widom, *Phys. Rev.* D **68**, 083004 (2003).
29. C. D. Dermer, *Astrophys. J.* **574**, 65 (2002).

30. M. Vietri, *Astrophys. J.* **453**, 883 (1995).
31. E. Waxman, *Phys. Rev. Lett.* **75**, 386 (1995).
32. M. Vietri, D. De Marco and D. Guetta, *Astrophys. J.* **592**, 378 (2003).
33. D. F. Torres, G. E. Romero, T. M. Dame, J. A. Combi and Y. M. Butt, *Phys. Rept.* **382**, 303 (2003).
34. I. V. Moskalenko, A. W. Strong and O. Reimer, astro-ph/0402243.
35. F. Aharonian [HEGRA Collaboration], *Astron. Astrophys.* **370**, 112 (2001) [*AIP Conf. Proc.* **558**, 749 (2001)].
36. K. W. Weiler, N. Panagia, R. A. Sramek, S. D. van Dyk, M. J. Montes and C. K. Lacey, astro-ph/0002501.
37. B. Zhang and P. Meszaros, astro-ph/0311321.
38. J. van Paradijs, C. Kouveliotou, and R. Wijers, *Ann. Rev. Astron. Astrophys.* **38**, 379 (2000).
39. D. A. Frail *et al.*, *Astrophys. J.* **562**, L55 (2001).
40. J. R. Hörandel, *Astropart Phys.*, in press [astro-ph/0402356].
41. K.-H. Kampert *et al.*, in: 27th International Cosmic Ray Conference (Copernicus Gesellschaft, Hamburg, Germany) Invited, Rapporteur, and Highlight Papers, P. 240 (2001).
42. E. Roulet, astro-ph/0310367.
43. A. M. Atoyan, F. A. Aharonian, H. J. Völk, *Phys. Rev.* D **52**, 3265 (1995).
44. A. W. Blain *et al.*, *Mon. Not. Roy. Astron. Soc.* **309**, 715 (1999).
45. D. J. Bird *et al.* [HIRES Collaboration], *Phys. Rev. Lett.* **71**, 3401 (1993).
46. C. D. Dermer and A. Atoyan, *Phys. Rev. Lett.* **91**, 071102 (2003).
47. G. Medina Tanco, in these Proceedings.
48. J. P. Rachen and P. Meszaros, *Phys. Rev.* D **58**, 123005 (1998).
49. G. Pugliese, H. Falcke, Y. Wang and P. L. Biermann, astro-ph/0003025.
50. P. L. Biermann, G. A. Medina-Tanco, R. Engel and G. Pugliese, astro-ph/0401150.
51. L. A. Anchordoqui, H. Goldberg, F. Halzen and T. J. Weiler, astro-ph/0311002.
52. G. Preparata, R. Ruffini and S. S. Xue, *Astron. Astrophys.* **338**, L87 (1998).
53. T. Damour and R. Ruffini, *Phys. Rev. Lett.* **35**, 463 (1975).
54. R. Ruffini, in these Proceedings. See also, R. Ruffini, C. L. Bianco, P. Chardonnet, F. Fraschetti and S. S. Xue, *Astrophys. J.* **581**, L19 (2002); C. L. Bianco, R. Ruffini and S. S. Xue, *Astron. Astrophys.* **368**, 377 (2001); R. Ruffini, J. D. Salmonson, J. R. Wilson and S. S. Xue, *Astron. Astrophys.* **350**, 334 (1999).
55. P. Chardonnet, A. Mattei, R. Ruffini, C. L. Bianco, F. Fraschetti, L. Vitagliano, S. -S. Xue, in these Proceedings.
56. M. Nagano *et al.*, *J. Phys.* G **18**, 423 (1992).
57. M. Takeda *et al.*, *Phys. Rev. Lett.* **81**, 1163 (1998); http://www-akeno.icrr.u-tokyo.ac.jp/AGASA ; date: February 24, 2003.
58. T. Abu-Zayyad *et al.* [HiRes Collaboration], astro-ph/0208243; astro-ph/0208301.
59. V. S. Beresinsky and G. T. Zatsepin, *Phys. Lett.* B **28**, 423 (1969); *Sov. J. Nucl. Phys.* **11**, 111 (1970) [*Yad. Fiz.* **11**, 200 (1970)].
60. Z. Fodor, S. D. Katz, A. Ringwald and H. Tu, in these Proceedings [hep-ph/0402102].
61. F. W. Stecker, *Astrophys. J.* **228**, 919 (1979); C. T. Hill and D. N. Schramm, *Phys. Rev.* D **31**, 564 (1985); C. T. Hill, D. N. Schramm and T. P. Walker, *Phys. Rev.* D **34**, 1622 (1986); F. W. Stecker, C. Done, M. H. Salamon and P. Sommers, *Phys. Rev. Lett.* **66**, 2697 (1991) [Erratum-ibid. **69**, 2738 (1991)]; S. Yoshida and M. Teshima, *Prog. Theor. Phys.* **89**, 833 (1993); R. J. Protheroe and P. A. Johnson, *Astropart. Phys.* **4**, 253 (1996); S. Yoshida, H. Y. Dai, C. C. H. Jui and P. Sommers, *Astrophys. J.* **479**,

547 (1997); R. Engel and T. Stanev, *Phys. Rev.* D **64** (2001) 093010; O. E. Kalashev, V. A. Kuzmin, D. V. Semikoz and G. Sigl, *Phys. Rev.* D **66**, 063004 (2002); Z. Fodor, S. D. Katz, A. Ringwald and H. Tu, *JCAP* **0311**, 015 (2003).
62. J. Bordes, H. M. Chan, J. Faridani, J. Pfaudler and S. T. Tsou, hep-ph/9705463; *Astropart. Phys.* **8**, 135 (1998).
63. G. Domokos, S. Kovesi-Domokos and P. T. Mikulski, hep-ph/0006328.
64. G. Domokos and S. Kovesi-Domokos, *Phys. Rev. Lett.* **82**, 1366 (1999); S. Nussinov and R. Shrock, *Phys. Rev.* D **59**, 105002 (1999); P. Jain, D. W. McKay, S. Panda and J. P. Ralston, *Phys. Lett.* B **484**, 267 (2000); A. V. Kisselev and V. A. Petrov, hep-ph/0311356.
65. M. Kachelriess and M. Plümacher, *Phys. Rev.* D **62**, 103006 (2000); L. Anchordoqui, H. Goldberg, T. McCauley, T. Paul, S. Reucroft and J. Swain, *Phys. Rev.* D **63**, 124009 (2001).
66. E. J. Ahn, M. Cavaglia and A. V. Olinto, *Phys. Lett.* B **551**, 1 (2003); P. Jain, S. Kar, S. Panda and J. P. Ralston, *Int. J. Mod. Phys.* D **12**, 1593 (2003).
67. L. A. Anchordoqui, J. L. Feng and H. Goldberg, *Phys. Lett.* B **535**, 302 (2002).
68. G. Domokos and S. Nussinov, *Phys. Lett.* B **187**, 372 (1987).
69. S. Barshay and G. Kreyerhoff, *Eur. Phys. J.* C **23**, 191 (2002); *Phys. Lett.* B **535**, 201 (2002); S. Kovesi-Domokos and G. Domokos, hep-ph/0307098; hep-ph/0307099.
70. H. Aoyama and H. Goldberg, *Phys. Lett.* B **188**, 506 (1987); A. Ringwald, *Nucl. Phys.* B **330**, 1 (1990); O. Espinosa, *Nucl. Phys.* B **343**, 310 (1990); V. V. Khoze and A. Ringwald, *Phys. Lett.* B **259**, 106 (1991).
71. D. A. Morris and R. Rosenfeld, *Phys. Rev.* D **44**, 3530 (1991); D. A. Morris and A. Ringwald, *Astropart. Phys.* **2**, 43 (1994).
72. A. Ringwald, *Phys. Lett.* B **555**, 227 (2003); *JHEP* **0310**, 008 (2003).
73. D. V. Semikoz and G. Sigl, hep-ph/0309328.
74. A. W. Strong, I. V. Moskalenko and O. Reimer, astro-ph/0306345; U. Keshet, E. Waxman and A. Loeb, astro-ph/0306442.
75. V. S. Berezinsky and A. Y. Smirnov, *Phys. Lett.* B **48**, 269 (1974); C. Tyler, A. V. Olinto and G. Sigl, *Phys. Rev.* D **63**, 055001 (2001); A. Kusenko and T. J. Weiler, *Phys. Rev. Lett.* **88**, 161101 (2002).
76. T. Han and D. Hooper, *Phys. Lett.* B **582**, 21 (2004).
77. H. Goldberg and T. J. Weiler, *Phys. Rev.* D **59**, 113005 (1999).
78. I. I. Balitsky and V. M. Braun, *Phys. Lett.* B **314**, 237 (1993); A. Ringwald and F. Schrempp, in: *Quarks '94*, Vladimir, Russia, 1994, hep-ph/9411217; S. Moch, A. Ringwald and F. Schrempp, *Nucl. Phys.* B **507**, 134 (1997); A. Ringwald and F. Schrempp, *Phys. Lett.* B **438**, 217 (1998); *Comput. Phys. Commun.* **132**, 267 (2000); *Phys. Lett.* B **503**, 331 (2001).
79. C. Adloff *et al.* [H1 Collaboration], *Eur. Phys. J.* C **25**, 495 (2002); S. Chekanov *et al.* [ZEUS Collaboration], hep-ex/0312048;
80. J. Abraham *et al.* [AUGER Collaboration], *Nucl. Inst. Meth.* A, in press.